

1	Results	2
1.1	Measurements at six modulation periods	2
1.2	Synchronizing the (1,1) series	5
1.3	3D behaviour of the self-similar and the square attractor	7
1.3.1	Phase propagation	7
1.3.2	Velocity	14

Results

The results that are discussed in this report are mainly the ones of the measurements of the square and the self-similar (1,1) attractor (with modulation periods of respectively 33.89 and 32.24 seconds). We looked at the variations of different parameters, mainly the phase, at different vertical and horizontal positions in the tank, to examine the 3D behaviour of the inertial waves. The data consisted of the velocities in two directions. To give an impression of the rough data, figure 1.1 shows the vectorfields of the self-similar (1,1) attractor during four moments in one modulation period. We can clearly see the attractor, represented by the largest arrows, which change of direction during a half period.

Measurements, though, have been done for other modulation periods too. To give an impression of the whole experiment, first some results are shown of all six modulation periods.

1.1 Measurements at six modulation periods

In this section, some examples are shown of measurements of vertical planes at the six modulation periods, which are already mentioned in chapter ???. The clearest way of visualizing the wave rays is by plotting $\sqrt{u^2 + w^2}$ as a representation of the in-plane kinetic energy. This is done in pictures 1.2-1.4. In each picture, $\sqrt{u^2 + w^2}$ is plotted at the moment in time, when the behaviour is the most clear. The distance to the front glass is chosen as 120 cm at all periods, because this is the location where the wave rays are best visible (as determined empirically).

- $\omega = 43.17s^{-1}$, first limit case: wave rays are parallel to the sloping wall.
- $\omega = 33.89s^{-1}$, square (1,1) attractor.
- $\omega = 32.24s^{-1}$, self-similar (1,1) attractor.
- $\omega = 29.97s^{-1}$, degenerate attractor.
- $\omega = 26.82s^{-1}$, (1,2) resonance.
- $\omega = 25.32s^{-1}$, (1,3) attractor.

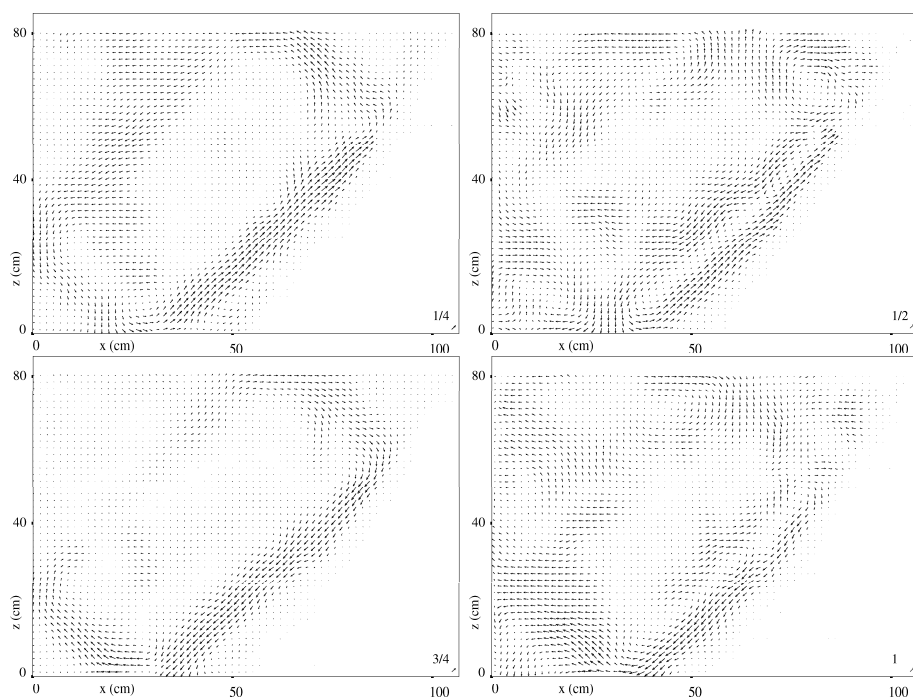


Figure 1.1: *Vectorfields of a vertical sheet at 120 cm from the front glass of the self-similar attractor at four moments during one period ($\frac{1}{4}$, $\frac{1}{2}$, $\frac{3}{4}$ and 1 period). The line of low velocity at $\frac{1}{2}$ and 1 period, near the sloping wall, will be explained in section ??.*

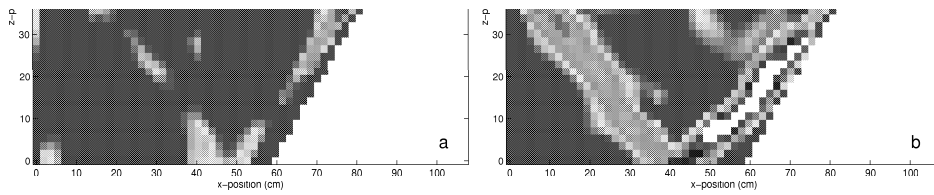


Figure 1.2: Kinetic energy of the limit case (a) and the square attractor (b). Horizontal (x -direction) and vertical (z -direction) distances are in centimetres, the in-plane energy ($\sqrt{u^2 + w^2}$) is in cm/s.

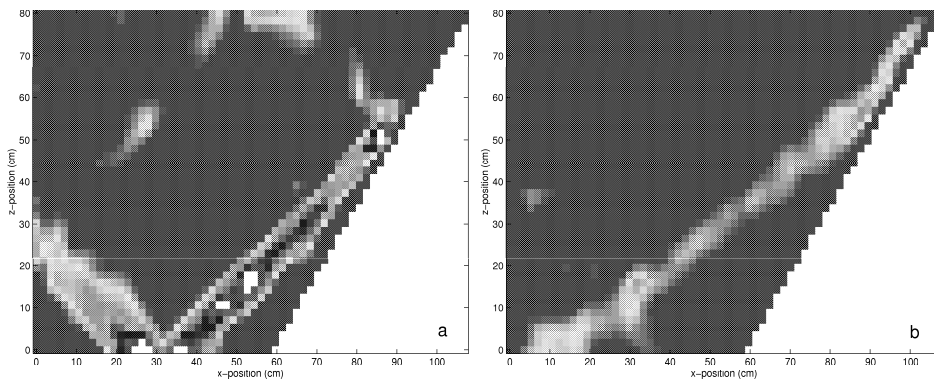


Figure 1.3: Kinetic energy of the self-similar attractor (a) and the degenerate attractor (b).

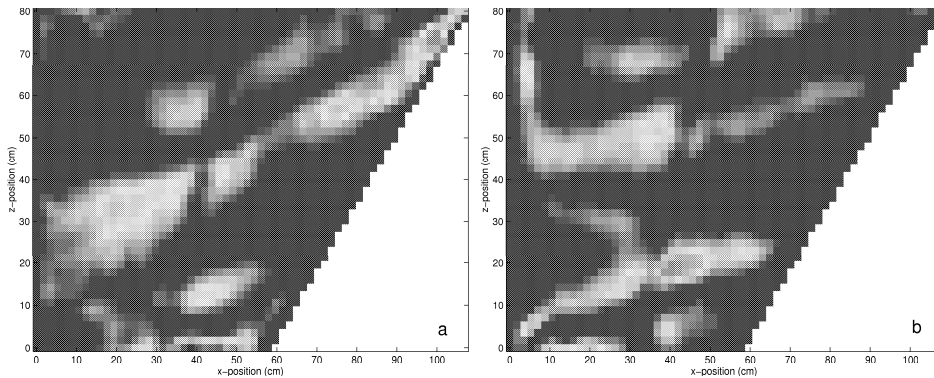


Figure 1.4: Kinetic energy of the (1,2) resonance (a) and the (1,3) attractor (b).

explain the line of high energy, from halfway the vertical wall to the acute corner.

The (1,3) attractor is not well visible because the container is relatively small, compared to the thickness of the rays. Furthermore, the resolution of the computer program CIVit could not make it possible visualizing more than 62 by 46 gridpoints, which is not enough to visualize complex behaviour. We can though see difference in the angles of the wave rays, and we can also visualize some of the ray pattern.

1.2 Synchronizing the (1,1) series

In section 1.3, we will look at the measurements of the self-similar and the square attractor and compare these with theory. We will try to obtain a 3D picture of the data, by comparing measurements of vertical sheets on different distances from the front glass. For this purpose, we want all series to start at the same moment in one modulation period, which was not the case for the original raw data. This is called 'synchronizing the series' and will be explained in this section.

For synchronizing we used the fact, that the vorticity-conserving, horizontal elliptic flow changes sign at the same moment over the whole container. This horizontal flow can be located by looking at the mean velocity in the x -direction. The moment of turning of the mean u -flow (velocity in the x -direction) over the whole xz -plane must be the same on all y -positions (see schematic picture 1.5). In the first picture, u is negative at all y (where $y < \frac{1}{2}L$). In the second, u is positive at all y . When we look at the other side of the container (thus when we place a wall at the right side, and the flow is forced to turn back), in this right half u will be positive in the first, and negative in the second picture. But, because our camera registered always at the same y -position, at about one quarter of the length of the tank, we do not need to take this into account.

The measurements of the horizontal flow are best visible in the horizontal xy -plane. In figures 1.6 and 1.7, the vectorfields of the horizontal net flow at two different heights are plotted. This is done at two opposite moments in one period of the self-similar attractor. The difference in dimensions in the x -direction of the vectorfields at the two heights is due to sloping wall.

We thus have seen that the mean horizontal velocity of the measurements of the vertical sheets can be used to synchronize the series at different y -distances. Herefor, the mean u -velocity at one y position is plotted with respect to the

moments in one modulation period.

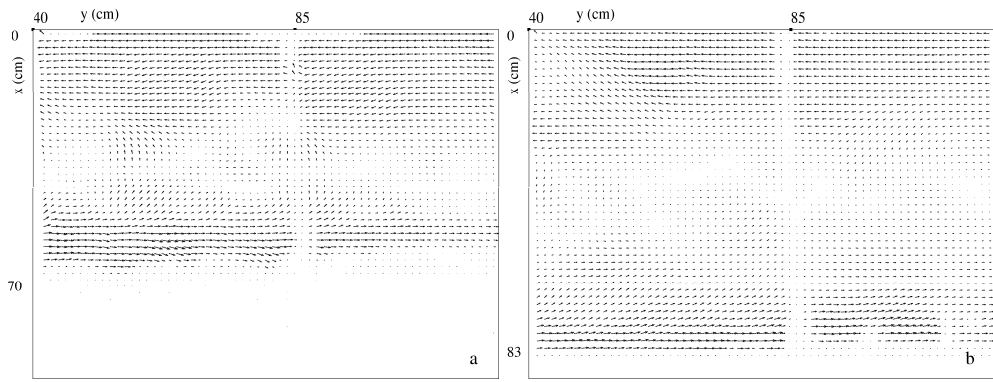


Figure 1.6: *Horizontal elliptic flow of the self-similar attractor, at a certain moment at two different heights (23 cm (a) and 43 cm(b)) from the bottom. The first plane has dimensions of 135.9×68.9 cm at 39.5 cm from the front wall. The second has dimension of 128.6×82.3 cm, also at 39.5 cm from the front wall. The line at $y = 85$ cm, with the small velocity components, is caused by the frame of the glass planes, that lied on top of the tank.*

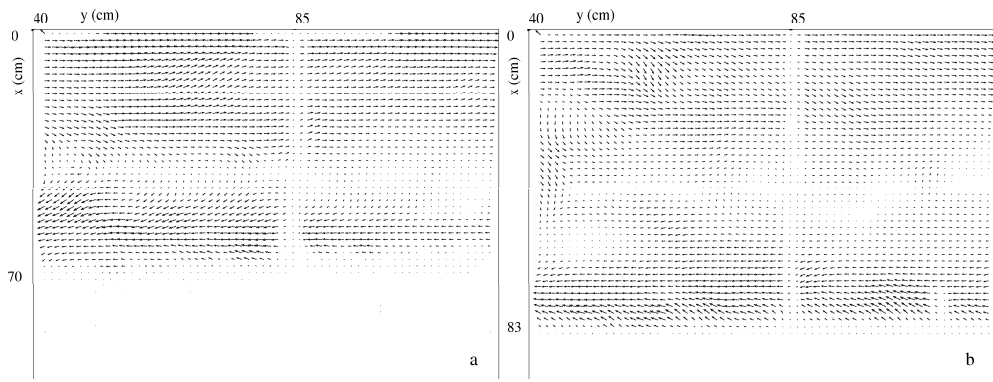


Figure 1.7: *The horizontal flow of figure 1.6 at half a period later. Here, the direction of the vectors is opposite to the directions in figure 1.6.*

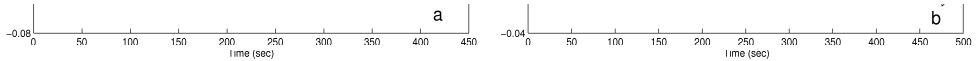


Figure 1.8: *Harmonical analysis of the mean velocity in the x -direction of the self-similar attractor at (a) 60 cm and (b) 150 cm of the front wall. The solid line represents the measurements, the dotted line the harmonical fit.*

time. This is represented by a sine, with a period that corresponds to the period of the modulation. With harmonical analysis, the phase of this sine can be calculated. See figure 1.8, where, with the solid line, the mean velocity in the x -direction of the self-similar attractor is plotted with respect to the time, at the y -positions of (a) 60 and (b) 150 cm from the front wall. The dotted line is the harmonical fit of the measurements. When we use this method for all y positions, the series can be shifted such that they all have the same phase, by letting all series start at different moments in time.

1.3 3D behaviour of the self-similar and the square attractor

1.3.1 Phase propagation

We already know, that the velocity vectors make one turn during a modulation period. When we observe a xz plane and we want to calculate the phase, we have to take into account, that we can only register a projection of the phase. Especially when the motion of the velocity is in a plane, which normal lies in the xz plane, the phase is not well defined. But this is the only thing we have, thus although this projection is not the real phase, we will refer to it as phase in the xz plane. This phase is calculated by

$$\phi = \arctan\left(\frac{w}{u}\right) \quad (1.1)$$

where we count whether the velocities are positive or negative, to be able to make a difference between both positive and both negative velocities.

Figure 1.9 is a schematic picture of the phase propagation (see [16]), which is perpendicular to the energy propagation, that is prescribed by the attractor and its convergence direction. The direction of the phase propagation (approaching or leaving the centre of the attractor) can be calculated from theory with the equations ?? and ?? (phase and group velocity). This phase propagation forms

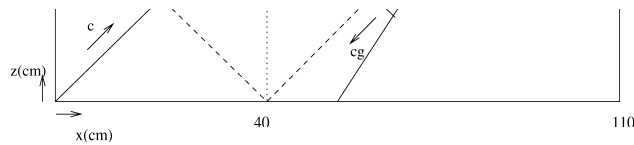


Figure 1.9: *Schematic picture of the directions of the phase- and the group-velocity. The square attractor is represented by the dashed line*

a saddle point.

The phase motion towards the sloping wall is very well visible in figures 1.1. At $\frac{1}{2}$ period and at 1 period, we can see a static line between two regions of high velocities, near the sloping wall, which thus can be explained by figure 1.9: phase propagation.

In figure 1.10, other measurements of the phase propagation are shown. We see twelve moments in one period of the square attractor, at a distance of 90 cm from the front wall, where a positive phase (thus between 0 and π) is coloured red, and a negative phase is blue. The motion of the phase is best visible in the lower left corner, where each region of equal phase (region of equal colour) is moving into the interne of the plane, which is equivalent with the schematical picture 1.9. A better view of the phase propagation is given by figure 1.11. These are also twelve moments in one period, but here the measurements of the self-similar attractor are used, at a distance $y = 60$ cm. Although the behaviour at this distance may not be ...representatief... for the whole container, the phase propagation is best visible here. In this figure, not only the phase propagation in the lower left corner is clear, but it is well visible in all areas.

Now, we have an impression of the phase motion in the xz -plane, but we do not know the variations in the y -direction, the $3D$ behaviour. Therefor, we examine the phase, first at a fixed x position and second at a fixed z position, with respect to the time, and we compare these figures at different y -positions. From figure 1.9, we can try to predict the behaviour of the phase at one y -position. When, for example, the line $x = 35$ cm is chosen, we expect an area of equal phase to move in positive z direction for small z , and a turning point near $z = 40$ cm (as is plotted in the schematical picture 1.9). We like to examine what happens at different y positions. In figures 1.12 an 1.13, the phase of the velocity vector, with respect to time, is plotted at one x or z position, at different horizontal y positions.

In these figures, the red part are the first measurements, wich have been re-

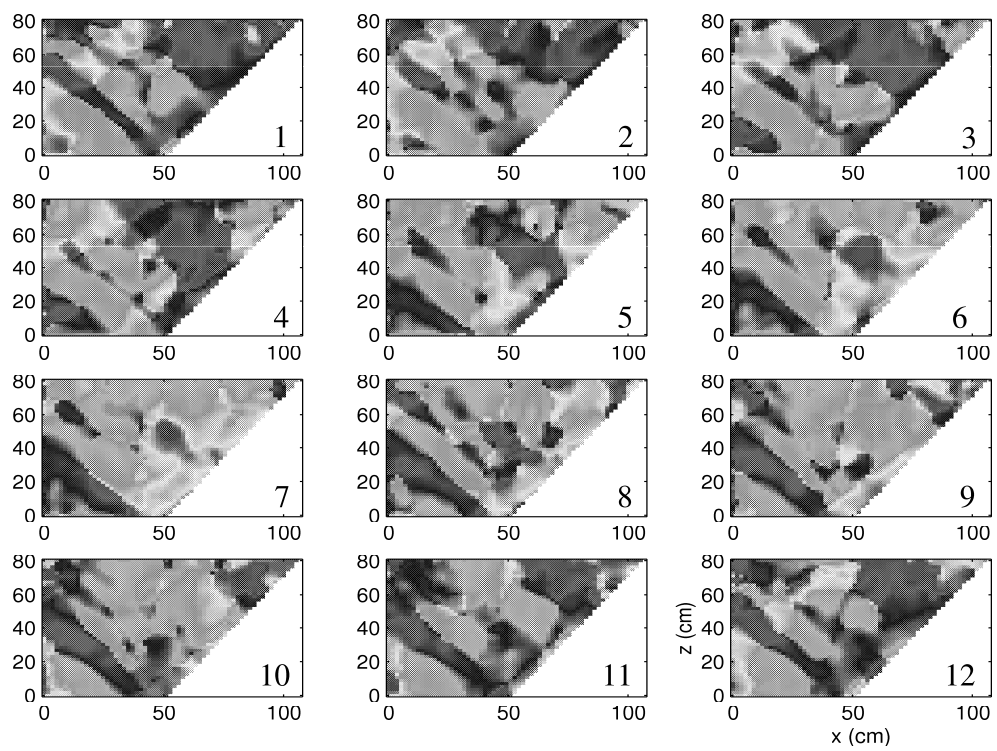


Figure 1.10: *Twelve moments in one period of the phase of the square attractor at a y -distance of 90 cm. The positive phase (thus between 0 and π) is coloured red, the negative phase is blue.*

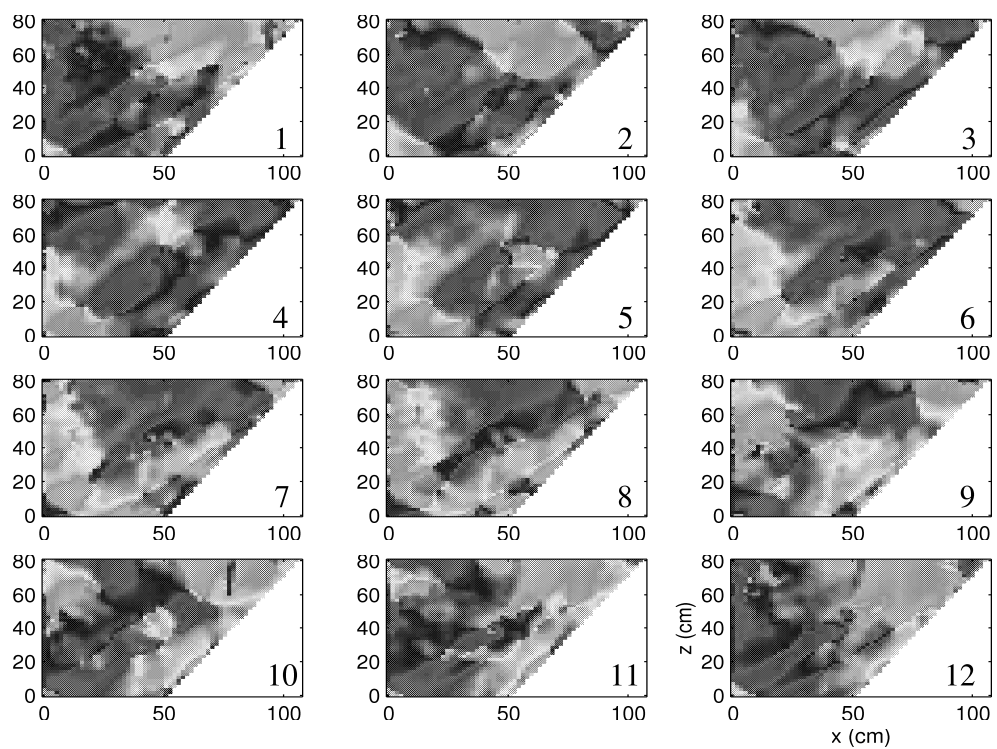


Figure 1.11: *Twelve moments in one period of the phase of the self-similar attractor at a y-distance of 60 cm. Time progress and phase colouring are the same as in figure 1.10.*

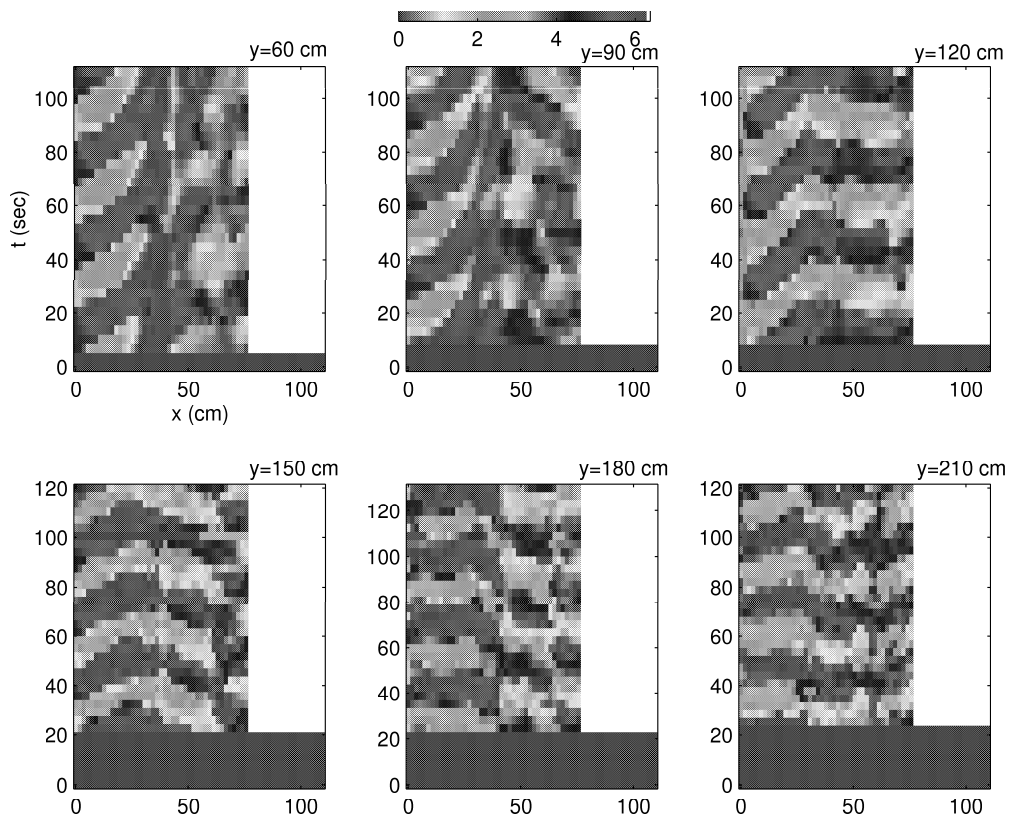


Figure 1.12: Phase of the velocity vector at $z = 35$ cm of the square (1,1) attractor. The new $t = 0$ lies at the line where the measurements begin.

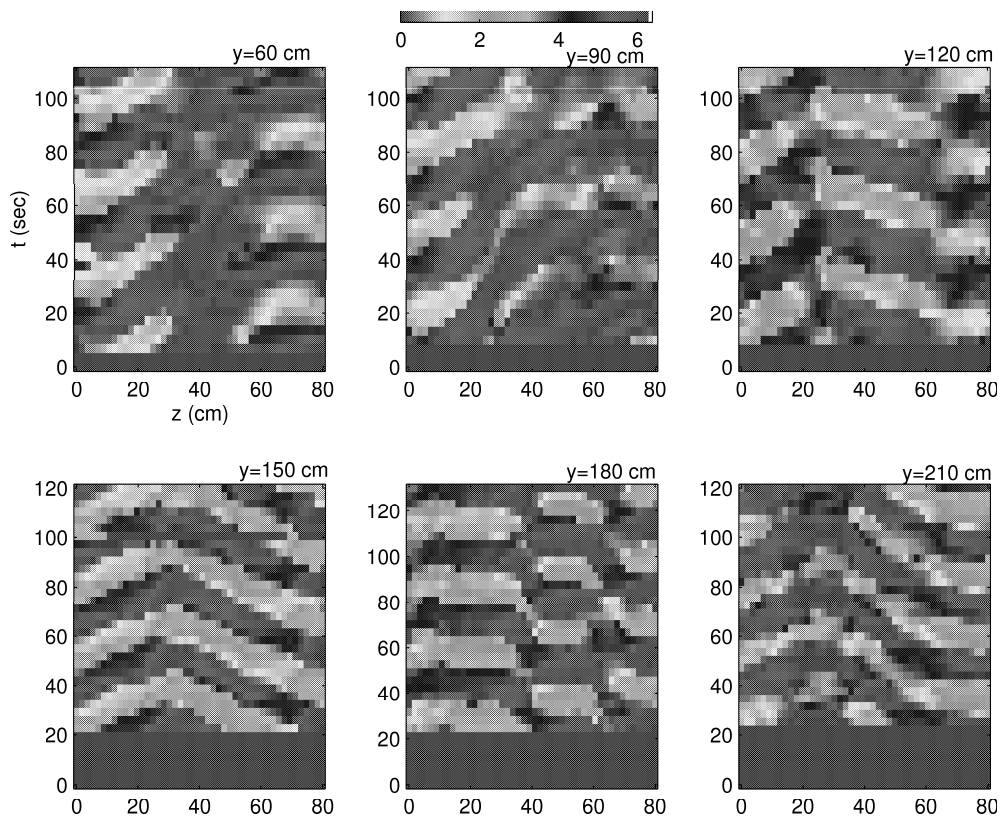


Figure 1.13: Phase of the velocity vector at $x = 35$ cm of the square $(1,1)$ attractor. The new $t = 0$ lies at the line where the measurements begin.

with figure 1.9, where we can see that in the lower left part of the xz plane, the phase moves in the right upward direction. This motion can be seen in all y positions, but the lines of equal phase are steeper in the first figures, close to the front wall, than in the planes in the centre of the tank. This means that the phase propagation in the horizontal (x) direction either changes its direction or changes its velocity with respect to the y direction.

Because the phase propagation keeps its velocity, throughout the tank (as seen in the theoretical results in chapter ??), figure 1.12 indicates that the phase velocity changes of direction. Because the direction of the phase velocity is perpendicular to the direction of the group velocity (which is the direction of the wave rays, that form the attractor), this indicates that the shape of the attractor changes, throughout the tank. From theory, we also know that at a fixed frequency, the angle of the direction in which energy propagates does not change. Apparently the theory of inertial waves does not suffice to explain this symptom.

The theory of other waves in enclosed rotating fluids, discussed in chapter ??, may give us an explanation for this behaviour. The inertial Poincaré waves, for instance, have a phase propagation that is perpendicular to the xz plane, in a positive y direction at large/small x and a negative y direction at small/large x . It turns at the front wall, where the phase velocity decreases in the y direction and increases in the x direction. This may explain the steeper lines of equal phase in figure 1.12: the phase propagation in the x direction changes of velocity, due to the inertial Poincaré waves.

Another obvious property of figure 1.12 is the fact that the phase seems to be shifted a half period at the first y position (60 cm), compared to the others, which have more or less the same phase, at the same (synchronized) time. It looks as if the turning velocity vectors at $y = 60$ cm ‘stick’ to the front wall, and are turning somewhat ‘later’ (or perhaps earlier) than the velocity vector in the interior of the tank.

The last property of figure 1.12 is the behaviour to the right of $x = 40$ cm. Here, the difference in the y direction is less well visible, because most of the pictures are unclear. This region is where the attractor reflects at the sloping wall and the wave rays converge. Therefore this is a region of high mixing, which could be the reason of the unclear phase propagation.

When we compare figure 1.12 with 1.13, we see that the same phase shift at $y = 60$ occurs. Furthermore, in the figure of the vertical line $x = 35$ cm, the difference in steepness at the different y positions is not as clear as in the horizontal line. This can be understood by realizing that the inertial Poincaré waves do not change as much over a vertical line, as over a horizontal line (where they change

ting phase, with respect to the y direction, at a fixed point. We now do not look at the differences in time (thus the behaviour in the xz plane) at different y positions, but only at the variations of the phase at one point in the y -direction. We used all self-similar (1, 1) series for this (with y positions at roughly every 10 or 20 cm, from 60 cm to 290 cm from the front wall, where the whole tank has a length of 500 cm). First the series are synchronized in time, such that they all start at one fixed moment in a period. Now, the average phase of the rotating velocity vector at several points in a small area is plotted, with respect to the y position (thus as a point). This is done by subtracting the mean phase, averaged over all y positions. The existence of several measurement series at one y position explains the occurrence of several datapoints at the same y . Now we again are able to examine the 3D behaviour of the phase and we can compare phase changes at different small areas over the y direction of the tank.

First, an area in the attractor is chosen, at a part where the kinetic energy is high, thus near the sloping wall (see figure 1.14). Second, we studied an area in the attractor, but at a position in the upper left corner in the attractor, with little kinetic energy (see figure 1.15). The phase in an area outside the attractor is not well defined, thus showing these measurements will not give any useful information.

In figures 1.14 and 1.15, we can see the same as we have remarked from the xt and zt phase figures: at $y = 60$ cm, the phase of the velocity vector is shifted 180 degrees with respect to all other positions. Another obvious behaviour is the fact that halfway the container (thus at $y = 240$ cm and beyond), the phase is shifting again. The consequence of this may be that the hypothesis that the velocity vectors 'stick' to the wall is not right, there seems to be another property of the motion. This may be a sort of imaginary wall at the centre of the container, which separates the motion into two cells. But another explanation may be that the measurements of the planes halfway the tank are very unclear and the ...foutenmarge... becomes large, thus we also have to consider these points to be not very accurate.

The last thing, we can say about these figures, is that in figure 1.14 (points in the attractor where the energy is high), the phase in the interior (between $y = 60$ cm and $y = 250$ cm) is much more consistent than in the measurements in the 'low-energy' part of the attractor. These measurements in the upper left part of the attractor, do not more or less lie on a line, but show a kind of parabola.....

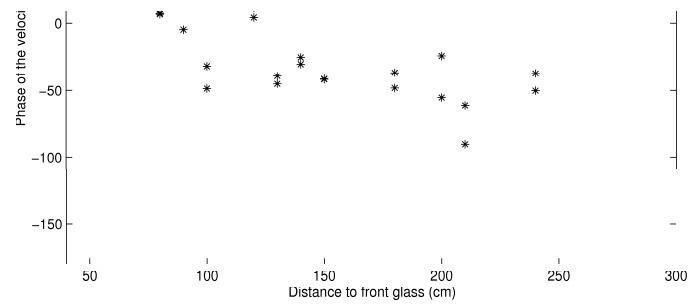


Figure 1.14: *Average phase of the velocity vectors at some points in an area of high energy in the attractor at different y positions throughout the container.*

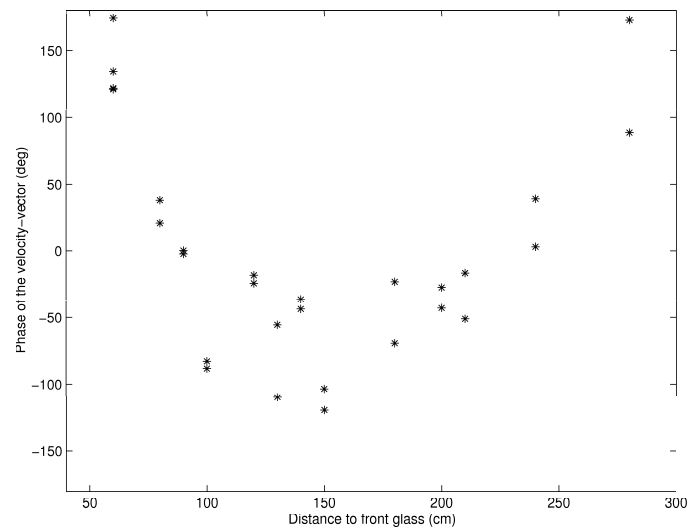


Figure 1.15: *Average phase of the velocity vectors at some points in an area of low energy in the attractor at different y positions throughout the container.*

creasing y (thus high energy near the front wall). We will further examine this later.

Furthermore, in the first figure, at $y = 60$ cm, the point of reflecting of the attractor at the bottom of the tank is shifted somewhat with respect to the other figures. The attractor at $y = 90$ cm is almost a square, in contrast with figure *a*. This shifting is probably due to the fact that the phase near the front wall is much different from the phase at all other y positions (as seen in section 1.3.1).

The last remark about the energy plots is about the difference between figure *a* and *b* in 1.17. In both plots, one of the sides of the attractor is not well visible. In the first (*a*), the upper left ray, is almost invisible, while in the second plot (*b*), the upper right ray can hardly be seen. The reason for this behaviour is still unknown.

The fact that the kinetic energy is decreasing in the direction of increasing y , is further examined. In figures 1.19 and 1.20, the amplitude (obtained with harmonical analyses) of the mean velocity in the whole plane is plotted with respect to the y distance. Figure 1.19 shows the amplitude of the mean u velocity and figure 1.20 the amplitude of the mean w velocity. We already discussed the horizontal u velocity and the fact that it changes of direction at the same moment over the whole container. The vertical velocity has a somewhat different behaviour. While this velocity is positive in one part of the attractor, it is negative in another part (and more or less equal to zero outside the attractor). This means that we expect the net vertical velocity, due to the influence of the inertial waves, to vanish.

When we plot the amplitudes of the mean velocities, it is clear that the vertical velocity does have an amplitude with a value that is comparable to the value of the amplitude of the mean horizontal velocity. Apparently, the modulation forces other kinds of waves (with the same frequency as the modulation frequency), which do have a mean vertical amplitude that is comparable to the mean horizontal amplitude, due to the inertial waves.

It is clear that the decreasing of kinetic energy ($\sqrt{u^2 + w^2}$) with increasing y (as seen in figures 1.16-1.18) is caused by the decreasing of the amplitude of w . In figure 1.20, we see an almost linear progress of the amplitude of w with y . The only exception is the point at $y = 290$, but here, probably the plotted value is very inaccurate. This linear behaviour can not be explained by the theory of other waves in enclosed rotating fluids as we have seen in chapter ???. To explain a behaviour as in figure 1.20, we may need more theoretical information about other waves that can appear.

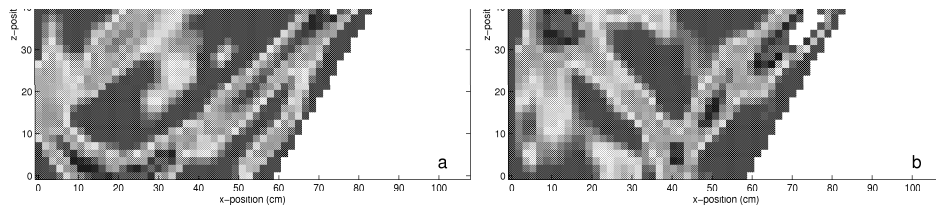


Figure 1.16: *Absolute velocity (or representation of the kinetic energy) of the self-similar (1,1) attractor. $\sqrt{u^2 + w^2}$ is in cm/s. Figure a is at 60 cm and b is at 90 cm from the front wall.*

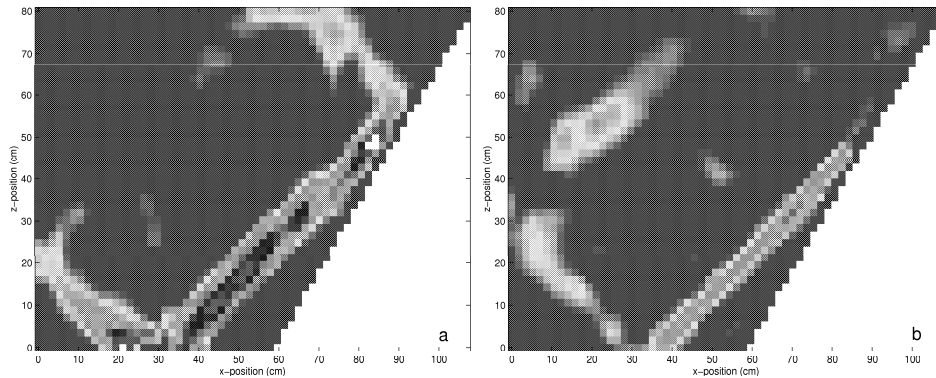


Figure 1.17: *Figure a is at 120 cm and b is at 150 cm from the front wall.*

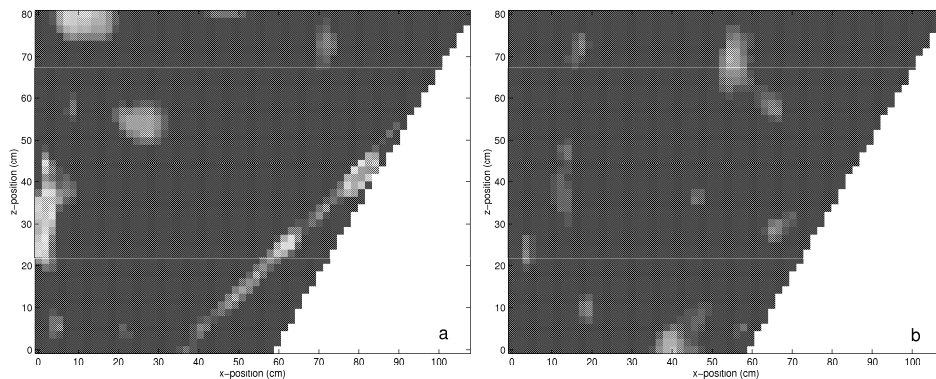


Figure 1.18: *Figure a is at 180 cm and b is at 210 cm from the front wall.*

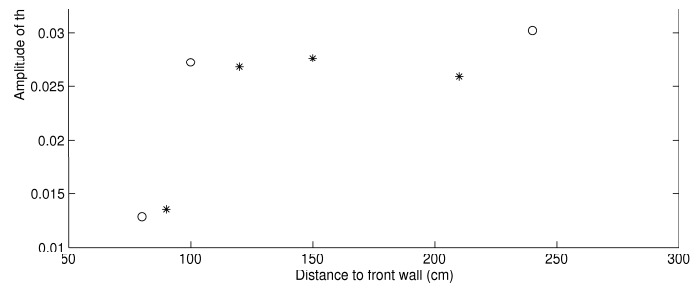


Figure 1.19: *Amplitudes of the mean horizontal velocities (over a xz plane) with respect to the y position. The stars and the dots are two series of measurements, taken at two different times, under somewhat different circumstances (like the number of particles or the number of bubbles).*

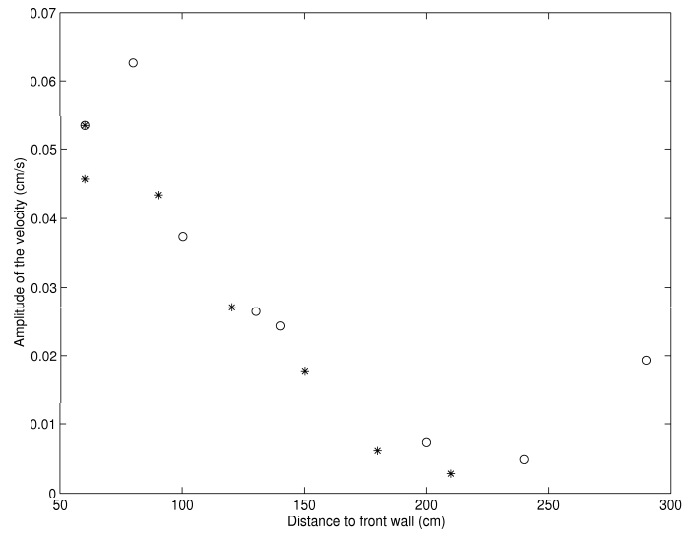


Figure 1.20: *Amplitudes of the mean vertical velocities (over a xz plane) with respect to the y position.*

outside of the attractor, in the centre of the tank).

In the first figure (1.21), in the attractor at a position with a high kinetic energy, we see a decline, with respect to the y position. The only exception is the point at $y = 290$ cm. But we do not pay much attention to this point, because the accuracy is very low. This behaviour is consistent with the behaviour in figure 1.20, the mean w velocity over the whole xz plane. The most obvious differences are the more linear progress of figure 1.20, and the last y position.

Furthermore, when we look at figure 1.22, we can see two points, at $y = 80$ cm and $y = 290$ cm, having a value much higher than the others, which all have about the same values. This behaviour is not consistent with figure 1.22. We can even see more similarity between figure 1.21 and figure 1.23 (the area where no attractor is appearing), where they both show a decline of amplitude with increasing y position and where they both have about the same values of the amplitudes. The last property is very remarkable, because we did not expect the waves to have a great velocity outside of the attractor. The explanation may again lie in the theory of other waves that appear in enclosed rotating fluids: the velocity pattern with amphidromic points, that is much different from the pattern of inertial waves, becomes important. Apparently, the 3D behaviour in this rotating container with one sloping wall is not only predictable by the theory of inertial waves, but there are other waves that have their influence on the behaviour of the fluid.

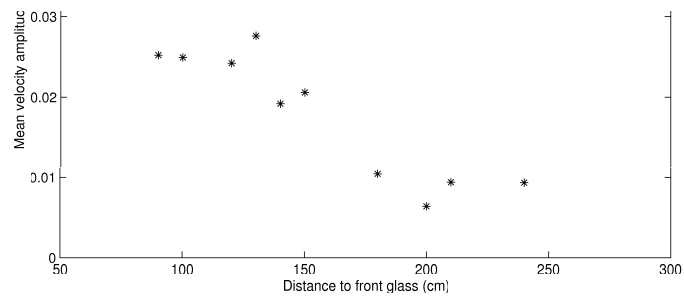


Figure 1.21: Length of the mean absolute velocity vectors at some points in an area of high kinetic energy in the attractor at different y positions throughout the container.

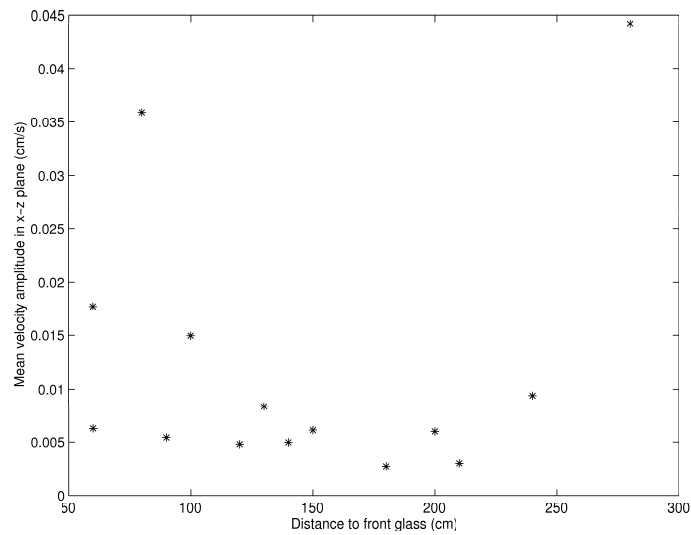


Figure 1.22: Length of the mean absolute velocity vectors at some points in an area of low kinetic energy in the attractor at different y positions throughout the container.

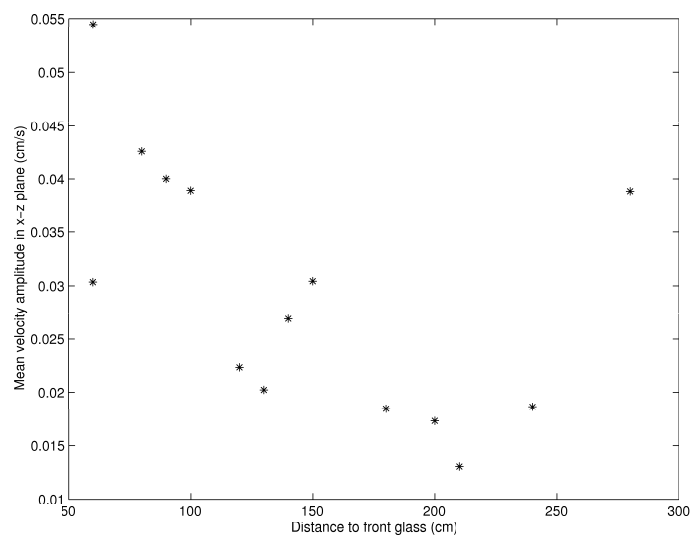


Figure 1.23: *Length of the mean absolute velocity vectors at some points in an area in the centre of the xz plane, outside the attractor at different y positions throughout the container.*

- [1] Pedlosky J., *Geophysical fluid dynamics*, Springer-Verlag New York, 2th edition, 1987.
- [2] Lighthill M.J., *Waves in fluids*, Cambridge University Press, 1978.
- [3] Tolstoy I., *Wave propagation*, McGraw-Hill, 1973.
- [4] Poincaré H., *Sur l'équilibre d'une masse fluide animée d'un mouvement de rotation*, Acta Math., **VII**, 259-380, 1885.
- [5] Maas L.R.M., Lam F.P.A., *Geometric focussing of internal waves*, J. Fluid Mech., **300**, 1-41, 1995.
- [6] Maas L.R.M., Benielli D., Sommeria J., Lam F.P.A., *Observations of an internal wave attractor in a confined, stably stratified fluid*, Nature, **388**, 7 august 1997.
- [7] Maas L.R.M., Verhulst F., Duistermaat J.J., *Appendix to Nonlinear Systems proposal: The dynamics of internal and inertial waves in enclosed basins*, 1998.
- [8] Greenspan H.P., *The theory of rotating fluids*, Cambridge University Press, 1964.
- [9] Boyce W.E., DiPrima R.C., *Elementary differential equations and boundary value problems*, John Wiley & Sons, 6th edition, 1997.
- [10] Tyn Myint-U *Partial differential equations for scientists and engineers*, , .
- [11] De Swart H., *Collegedictaat Lange golven en getijden*
- [12] LeBlond P.H., Mysak L.A., *Waves in the ocean*, Elsevier, 1978.
- [13] Open University Course Team *Ocean circulation*, The Open University inassociation with Pergamon Press, 1989.
- [14] Maas L.R.M., manuscript in preparation: *Inertial waves in enclosed, rotating fluids*, 2000.
- [15] Fincham A.M., Spedding G.R., *Low cost, high resolution DPIV for measurement of turbulent fluid flow*, Exp. in Fluids, **23**, 449-462, 1997.
- [16] Pörtzgen N., *Dataverwerking van metingen aan Inertiaalgolven*, 1998.